ISSN 1063-7826, Semiconductors, 2012, Vol. 46, No. 10, pp. 1326–1330. © Pleiades Publishing, Ltd., 2012.

FABRICATION, TREATMENT, AND TESTING OF MATERIALS AND STRUCTURES

Influence of Source-to-Substrate Distance on the Properties of ZnS Films Grown by Close-Space Sublimation[1]

M. Ashrat[a], M. Mehmood[a], and A. Qayyum[b]^

[a] *Department of Metallurgy and Materials Engineering, Pakistan Institute of Engineering and Applied Sciences, Islamabad 45650, Pakistan*

[b] *Physics Division, Pakistan Institute of Nuclear Science and Technology, P.O. Nilore, Islamabad 45650, Pakistan*

^e-mail: qayyum@pinstech.org.pk, aqayyum11@yahoo.com

Received June 30, 2011; in final form, March 15, 2012

Abstract—ZnS films were deposited on soda glass at various source-to-substrate distances by closespace sublimation. The influence of source-to-substrate distance on the structural and optical properties of the films was investigated. XRD spectra showed that films were crystalline in nature having cubic structure oriented mainly alogn (111) plan. The crystallinity of films increased with the source-to-substrate distance up to 40 mm. The crystallite size increases from 15.76 to 19.06 nm as the source-to-substrate distance increased from 5 to 40 mm. AFM data reveled that RMS roughness decreases and grain size of the film increases with the source-to-substrate distance. The optical transmittance in the visible range was about 70% for all films. The refractive index of a ZnS film decreases with increasing source-to-substrate distance. But source-to-substrate distance seems to have no effect on the energy bandgap and absorption edge of ZnS films. Moreover, it is shown that resisitivity of the ZnS films resuced significantly by Ag doping.

DOI: 10.1134/S106378261210003X

1. INTRODUCTION

ZnS is one of the famous II–VI compound semiconductor that is suitable for variety of optical applications including its use as a buffer layer in solar cells. The energy conversion efficiency of a solar cell depends also on the marerial of the buffer layer. So far highest energy conversion efficiency of a solar cell has been reported with the CdS buffer layer [1]. Despite the fact that CdS is a toxic material about 20% of incident photons are absorbed in buffer layer due to its narrow bandgap (~2.42 eV) [2]. In comparison with CdS, ZnS is environmental friendly and a wide bandgap material (~3.6 eV). Therefore ZnS is a prospective contender for the buffer layer of the upcoming family of solar cells. ZnS films have also several other applications in the area of light emitting diodes [3], electroluminescent devices [4], antireflection coating and optical filters [5, 6]. Previously, ZnS thin film have been deposited by thermal evaporation [7], electron beam evaporaiton [8], chemical vapor deposition [9], chemical bath deposition [10], pulsed laser deposition [11], molecular beam epitaxy [12] and close-space sublimation (CSS) [13]. In the present study we have prepared ZnS thin films by a modified closed space sublimation apparatus. In particular, the influence of source-to-substrate distance on the structural and optical properties has been systematically investigated.

[1] The article is published in the original.

2. EXPERIMENTAL SETUP

High purity (99.9%) ZnS powder was used as a source for deposition of ZnS films on soda lime glass substrates. The glass substrate were first treated with detergent and washed in running water. The substrates were then dried with a fine tissue paper and cleaned with isopropyol alcohol (IPA) in an ultrasonic cleaner. All the films were deposited by CSS technique, using a high vacuum coating unit. But our experimental set up was slightly different form the conventional CSS device. In conventional CSS device, the source to substrated distance in usually few millimeters, but we varied source to substrate up to 50 mm. The molybdenum boat was used as source for ZnS powder. A vacuum of $\leq 10^{-5}$ mbar was maintained in the chamber during deposition. The adhesion of the films deposited at room temperature was not good; therefore substrate temperature during deposition was kept 300°C. Structure of the films was determined by X-ray diffraction at room temperature by Bruker D8 diffractometer using CuK_α radiation in the scanning mode. The surface morphology of the films was investigated by atomic force microscope (AFM). Transmission of the films was measured in the range of 300–2500 nm using Perkin Elmer Lambda 19 UV/VIS/NIR spectrophotometer and UV Win Lab software. Thickness and refractive indices of these films were determined by fitting the transmittance data using Swanepoel model [14]. The dark dc resistivity of the ZnS films was measured at room temperature by two-probe method.

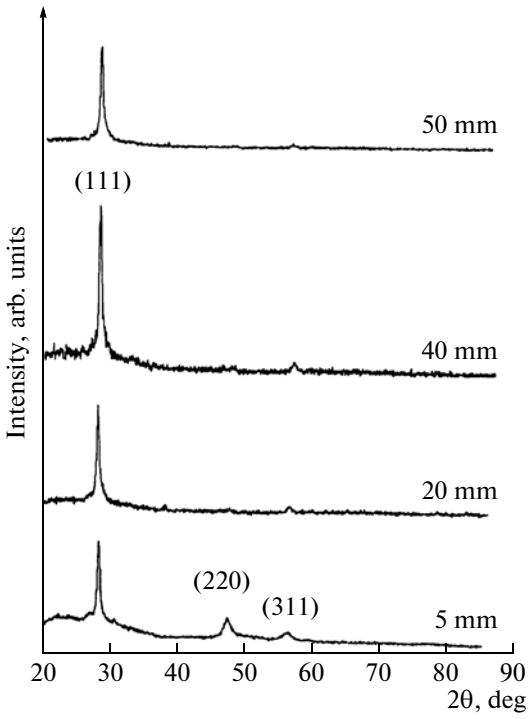

Fig. 1. XDR pattern of ZnS films deposited at various source-to-substrate distances.

3. RESULTS AND DISCUSSION

The ZnS films prepared by CSS at various source-to-substrate distances were pinhole free and strongly adherent to the substrate. The XDR profiles of ZnS films deposited at the source-to-substrate distance of 5, 20, 40 and 50 mm are shown in Fig. 1. It is observed that films are polycrystalline in nature having cubic crystal structure with the preferred orientated along (111) plane, other secondary peaks visible at 47.45° and 56.40° are due to (220) and (311) orientations of cubic ZnS. These results are in good quantitative agreement with the recent work of Prathap et al. [15] for ZnS films deposited by CSS technique. However, structure of ZnS films is known to depend on the deposition technique. For instance, thermally evaporated ZnS films are generally cubic [16, 17], ZnS films grown by sulfurizing of RF sputtered ZnO was hexagonal in nature [18] and films grown by spray pyrolysis had mixed cubic and hexagonal phases [19]. Figure 1 also shows that the intensity of (111) peak increases with the source-to-substrate distance up to 40 mm and then decreases. Whereas (220) and (311) peaks begin to disappear with increasing source-to-substrate distance. The effect of source-to-substrate distance on the full width at half maximum (FWHM) of (111) peak is shown in Fig. 2. The FWHM decreases with source-to-substrate distance up to 40 mm, which indicates the improvement in crystallinity of thee films.

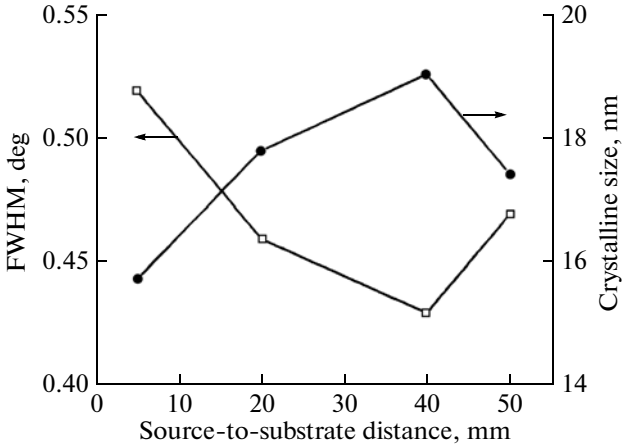

Fig. 2. Variation of FWHM of (111) peak and cystallite size as a function of source-to-substrate distance.

The average crystallite size, τ, was estimated using Scherrer formula [20]

$$\tau = \frac{K\lambda}{\beta\cos\theta}, \quad (1)$$

where K is the shape factor that was taken equal to 0.9, λ is the wavelength of X-ray source, β is the FWHM of (111) peak and θ is the Bragg diffraction angle in degree. The crystallite size of ZnS films increases from 15.76 to 19.06 nm as the source-to-substrate distance increased from 5 to 40 mm (see Fig. 2). Figure 3 shows AFM images of the films deposited at 5, 30 and 40 mm respectively. It can be seen that films are uniform, densely packed and pinhole free. RMS roughness of films reduces from 15 to 6 nm with increase of source-to-substrate distance. AFM images also revealed that the grain size increases with the increase of source-to-substrate distance.

For optical applications a films with high transmittance in the visible range is also important. The optical transmittance spectra of ZnS films deposited at the source-to-substrate distances of 20, 40 and 50 nm are shown in Fig. 4. It can be seen that the average transmittance in the 400–2500 nm wavelength range is about 70% for all films regardless of the source-to-substrate distance. The fluctuations in the transmittance spectra are probably due to the interference originated from the reflection at interfaces in the films. It was also observed that source-to-substrate distance do not have any effect on the position of absorption edge. The energy band gap of ZnS films were calculated using the Tauc relation [21] in which a graph $(\alpha h\nu)^2$ vs. $h\nu$ is plotted. Where a is the absorption coefficient and $h\nu$ is the photon energy. The absorption coefficient α was determined from the transmittance T as $T = e^{-\alpha x}$, where x is thickness of the film. The energy band gap E_g was determined by extrapolation of the

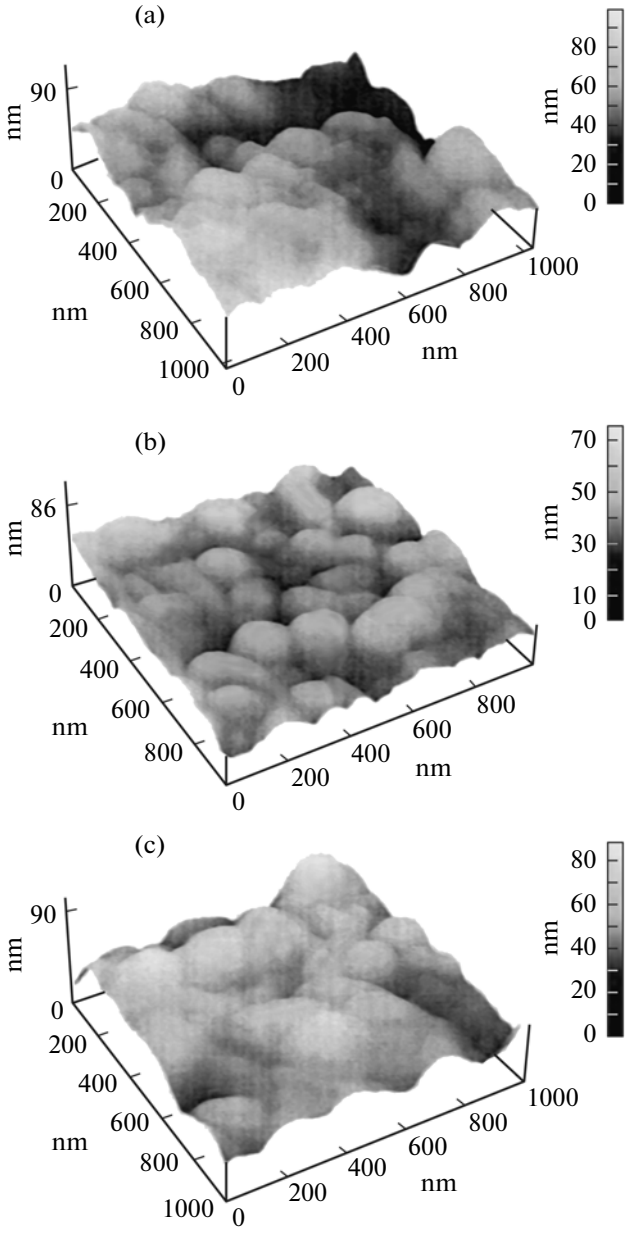

Fig. 3. AFM images of ZnS films deposited at various source-to-substrate distances.

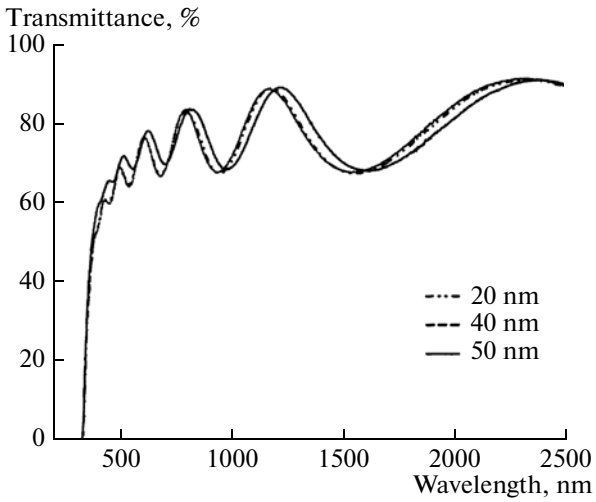

Fig. 4. Transmission of ZnS films deposited at various source-to-substrate distances.

linear portion of $(\alpha h\nu)^2$ vs. $h\nu$ curves to $(\alpha h\nu)^2 = 0$ (see Fig. 5). The variation of E_g as a function of the source-to-substrate distance is also plotted in Fig. 5. It can be seen that E_g is not sensitive to the source-to-substrate distance.

Thickness and refractive index, n, of ZnS films were calculated by fitting the transmission spectra using the following relation [14]

$$T = \frac{Ax}{B - Cx\cos\phi + Dx^2}, \qquad (2)$$

where T is the normal transmittance,

$$A = 16n^2 s, \quad B = (n+1)^3(n+s^2),$$
$$C = 2(n^2-1)(n^2-s^2),$$
$$D = (n-1)^3(n-s^2), \quad \phi = 4\pi nd/\lambda,$$
$$x = \exp(-\alpha d)$$

and

$$k = \alpha\lambda/4\pi.$$

Here, s is the refractive index of the glass substrate. The n and α both vary with wavelength as

$$n = a + b/\lambda^2 \quad \text{and} \quad \alpha = c + f/\lambda + s/\lambda^2,$$

respectively [14, 22]. Where a, b, c, f and g are constants. Considering all the multiple reflections at the interface for the case of $k^2 \ll n^2$, which is true for this kind of semiconductor thin film, Eq. (1) provides good fitting in transparent as well as in medium absorption region. Thickness of various films was in the range of 516 to 549 nm. The refractive index of three ZnS thin films deposited at various source-to-substrate distances is plotted as a function of wavelength in Fig. 6. Following trends can be deduced from these investigation: (i) the refractive index of a ZnS film decreases with increasing source-to-substrate distance that may be due to the reduction of tensile stresses in the films deposited at higher source-to-substrate distance [23], (ii) the refractive indices of all films are higher at shorter wavelengths and (iii) decreases with increase of the wavelength towards infrared region (IR). The values of refractive index and trends (ii) and (iii) are in good agreement to that of ZnS films deposited by Wu et al. [24] using evaporation. The controlled variation in the refractive index of ZnS films by adjusting

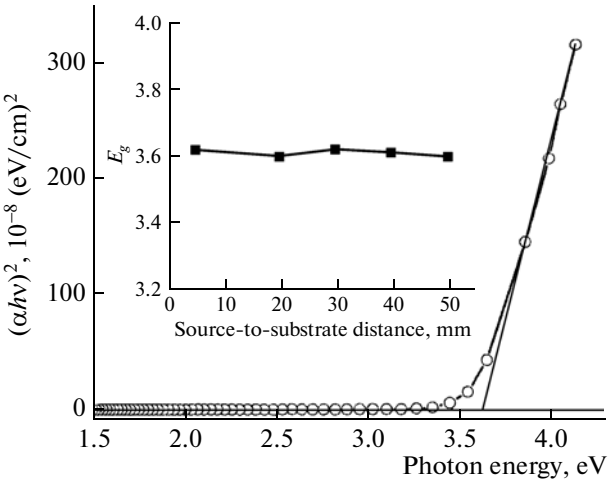

Fig. 5. The $(\alpha h\nu)^2$ versus photon energy for a ZnS film deposited at source-to-substrate distance of 40 mm. Inset shows energy bandgap of ZnS films as a function of source-to-substrate distance.

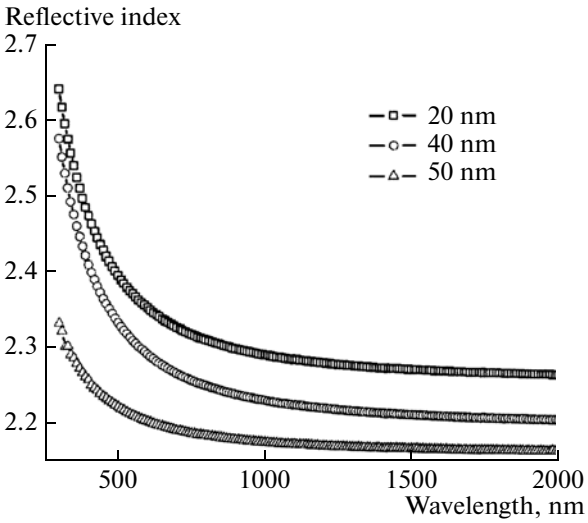

Fig. 6. Refractive index of ZnS films deposited at various source-to-substrate distances.

source-to-substrate distance may be useful for designing an optical coatings for a particular application.

As-deposited films showed resistively of the order of 10^8 Ω cm. The high resistivity of the as-deposited films indicates that films are highly stoichiometric. The highly resistive ZnS film can be used as a buffer layer in solar cells. Whereas the application of ZnS films can be extended in the filed of optoelectronics by reducing their resistivity, particularly where low series resistance are required for fabrication of photodiodes, display screens and other optoelectronic devices [15]. In order to reduce the resistivity, ZnS films deposited at source-to-substrate distance of 40 mm were immersed in silver nitrate solution for different times

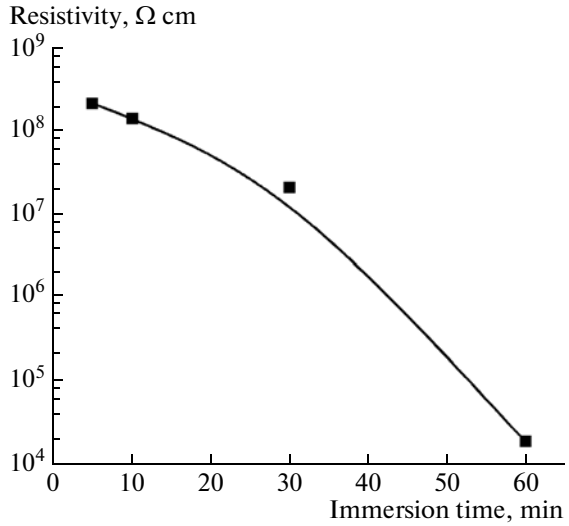

Fig. 7. Resistivity verses immersion time of Ag doped ZnS films.

and then heat treated in vacuum for one hour at 400°C. It can be seen in Fig. 7 that the resistivity of ZnS film consistently decreases with immersion time and resistivity of the ZnS film immersed in silver nitrate solution for 60 min was reduced by 4 orders of magnitude. We attribute reduction of resistivity to the increase of Ag diffusion in the films with immersion time. The measurements performed with the hot probe revealed that Ag-doped ZnS films has *p*-type conductivity.

4. CONCLUSIONS

The effect of source-to-substrate distance on the structural and optical properties of ZnS films deposited by CSS has been investigated. The crystallinity of the films showed improvement with the increasing source-to-substrate distance up to 40 mm. AFM data reveled that RMS roughness decreases and grain size of the film increases with the source-to-substrate distance. Optical studies of the ZnS films showed about 70% transmittance in the visible range and a significant decrease in the refractive index with increasing source-to-substrate distance. But source-to-substrate distance seems to have no effect on the energy bandgap and absorption edge of ZnS films. As-grown films showed a high resistivity (~10^8 Ω cm) that dropped to 2×10^4 Ω cm by Ag doping and annealing.

REFERENCES

1. K. Ramanmathan, M. Contreras, C. L. Perkin, S. Asher, F. S. Hasoon, J. Keane, D. Young, M. Romero, W. Metzger, R. Noufi, J. Ward, and A. Duda, Progr. Photovolt.: Res. Appl. **11**, 225 (2003).

2. S. Armstrong, P. K. Datta, and R. W. Miles, Thin Solid Films **403–404**, 126 (2002).
3. S. Yamaga, A. Yoshokawa, and H. J. Kasain, Cryst. Growth **86**, 252 (1998).
4. J. Vidol, O. de Melo, O. Vigil, N. Lopez, G. C. Puent, and O. Z. Angle, Thin Solid Films **419**, 118 (2002).
5. J. A. Ruffner, M. D. Hilmel, V. Mizrahi, G. I. Stegeman, and U. J. Gibson, Appl. Opt. **28**, 5209 (1989).
6. M. A. Ledger, Appl. Opt. **18**, 2979 (1979).
7. X. W. F. Lai, L. L. J. Lv, B. Zhuang, Q. Yan, and Z. Huang, Appl. Surf. Sci. **254**, 6455 (2008).
8. S. Wang, X. Fu, G. Xia, J. Wang, J. Shao, and Z. Fan, Appl. Surf. Sci. **252**, 8734 (2006).
9. Q. J. Feng, D. Z. Sheen, J. Y. Zhang, H. W. Liang, D. X. Zhao, Y. M. Lu, and X. W. Fan, J. Cryst. Growth **285**, 561 (2005).
10. P. Roy, J. R. Jota, and S. K. Srivastava, Thin Solid Films **515**, 1913 (2006).
11. K. H. Hillie and H. C. Swart, Appl. Surf. Sci. **253**, 8513 (2007).
12. M. Yokoyama, K. I. Kashiro, and S. I. J. Ohta, Cryst. Growth **81**, 73 (1987).
13. Y. P. V. Subbaiah, P. Prathap, and K. T. R. Reddy, Appl. Surf. Sci. **253**, 4909 (1987).
14. R. J. Swanepoel, Phys. E: Sci. Instrum. **16**, 1214 (1983).
15. P. Prathap, N. Revathi, Y. P. V. Subbaiah, K. T. R. Reddy, and R. W. Miles, Solid State Sci. **11**, 224 (2009).
16. G. Gordillo and E. Romero, Thin Solid Films **484**, 352 (2005).
17. M. Ashraf, S. M. J. Akhtar, M. Mehmood, and A. Qayyum, Eur. Phys. J. Appl. Phys. **48**, 10501 (2009).
18. R. Zhang, B. Wang, and L. Wei, Mater. Chem. Phys. **112**, 557 (2008).
19. A. El. Hichou, M. Addou, J. L. Bubendorff, J. Ebothe, B. El. Idrissi, and M. Troyon, Semicond. Sci. Technol. **19**, 230 (2004).
20. B. Cullity, *Elements of X-Ray Diffraction* (Addison–Wedley, London, 1959), p. 99.
21. J. Tauc, *Amorphous and Liquid Semiconductors* (Plenum, New York, 1974), p. 159.
22. R. J. Swanepoel, Phys. E: Sci. Instrum. **16**, 1214 (1983).
23. Y. P. V. Subbaiah, P. Prathap, and K. T. Ramakrishna Reddy, Appl. Surf. Sci. **253**, 2909 (2006).
24. X. Wu, F. Lai, L. Lin, B. Zhuang, Q. Yan, and Z. Huang, Appl. Surf. Sci. **254**, 6455 (2004).